

Supplementary Materials for

RIPK1 and NF-κB signaling in dying cells determines cross-priming of CD8⁺ T cells

Nader Yatim, Hélène Jusforgues-Saklani, Susana Orozco, Oliver Schulz, Rosa Barreira da Silva, Caetano Reis e Sousa, Douglas R. Green, Andrew Oberst, Matthew L. Albert*

*Corresponding author. E-mail: albertm@pasteur.fr

Published 24 September 2015 on *Science* Express
DOI: 10.1126/science.aad0395

This PDF file includes:

Materials and Methods
Figs. S1 to S11
Tables S1
Captions for Movies S1 to S3

Other Supporting Online Material for this manuscript includes the following: (available at www.sciencemag.org/cgi/content/full/science.aad0395/DC1)

Movies S1 to S3

Materials and Methods

Cells and constructs. Activatable RIPK3 chimeric proteins were constructed as previously described(21). Briefly, full-length mouse *ripk3* or *ripk3* lacking the final 42 amino acids (RIPK3ΔC) were cloned upstream of two copies of FKBP carrying the F36V mutation, herein called “FV” domains. These RIPK3-2xFV fusion proteins were cloned into pBabe-Puro retroviral vectors. Similarly, activatable Caspase-8 chimeric protein was generated by cloning human *caspase-8*, lacking the first 205 amino acids (ΔN-Caspase-8), downstream of one copy of FV domain. Additionally, ΔN-Caspase-8 and RIPK3ΔC were cloned upstream of a T2A ribosome-skipping sequences derived from porcine teschovirus-1 (EGRGSLLTCGDVEENPGP) followed by eGFP, creating bicistronic constructs in which our fusion protein and GFP are translated from the same mRNA. These constructs were transduced into NIH-3T3 cells (ATCC) using standard protocols for retroviral transduction. Transduced cells were selected for 5 days in 1 μ g/ml Puromycin, then grown to confluence and/or sorted for homogenous GFP expression. RIPK3-2xFV fusion protein was also cloned into a Tet-ON lentiviral plasmid (pSILK) and used to transduce NIH-3T3 using standard protocols for lentiviral transduction. Transduced cells were selected for 7 days in 200 μ g/ml hygromycin. Induction of target gene expression (RIPK3-2xFV) was done by treatment with doxycycline (500ng/ml) overnight. Dimerization of fusion proteins was induced by treatment with a specific drug ligand (AP20187, purchased from Clontech, BB homodimerizer) that is created by chemically linking two derivative molecules of FK506 in a manner that eliminated immunosuppressive activity and binding to endogenous FKBP, while still binding to FV proteins.

NIH-3T3 cell lines expressing death constructs (acC8, acR3 and acR3ΔC) were also transduced to express a truncated and non-secreted OVA–mcherry fusion protein (ΔOVA), or LifeAct (a 17-amino acid peptide that binds actin-filaments) ΔOVA fusion protein (LA-ΔOVA). Cells were sorted twice for homogenous mcherry (ovalbumin) expression between the cell lines. pBabe-GFP- I κ B(S32A, S36A) was purchased from addgene (#15624).

NIH-3T3 cells, B16-OVA F10 melanoma cells, mouse embryonic fibroblasts (MEFs) were cultured in DMEM (Gibco) supplemented with 10%FCS (PAA), 0.1 mM non-essential amino acids, 1mM sodium pyruvate, 10mM Hepes, 60 uM beta-mercaptoethanol and 0,02 mg/ml gentamycin (Gibco). CT-26 colon carcinoma cells (ATCC) and primary cells were cultured in RPMI (Gibco) supplemented as described for DMEM.

NIH-3T3 and CT26 lacking RIPK1 were created via stable transduction with a lentiviral vector encoding the Cas9 endonuclease, a guide RNA containing a targeting sequence specific for murine RIPK1, and a puromycin resistance cassette (a kind gift from Drs. Elizabeth Gray and Daniel B. Stetson). The sequence used to target RIPK1 was: GGGTCTTAGCACGTGCATC. Transduced cells were selected in puromycin, then cultured for 10 days to allow genome editing. Effective RIPK1 ablation was confirmed by western blotting.

Mice. WT C57BL/6 J CD45.2 Thy1.2 and BALB/c CBYJ mice were obtained from Charles Rivers, France. C57BL/6 J *batf3*^{-/-} transgenic mice were purchased from Jackson laboratory and bred in our mouse facility. 7-12 weeks old female mice were used. Mice were maintained in a specific pathogen free facility and all experimental protocols were approved by the Comité d'éthique pour l'expérimentation animale (The Ethics Committee for animal experimentation), Paris.

In vivo cross-priming assay. Indicated cell lines were harvested and resuspended in complete media at 5×10^6 cell/ml. Dimerizer was added at 1 μ M and cells were incubated for 15 min at 37°C, gently flicking the tube every 5 min. Ice cold PBS was added and cells were washed, counted and resuspended in cold PBS at 10^7 cells/ml and kept on ice until injections. 100 μ L of cells (10^6 cells) were injected intra-dermally (i.d.) in the flank of the mice. 9 days later, the spleen and the draining lymph node (inguinal lymph node) were harvested, pooled and stained for surface markers. To analyse intracellular cytokine expression, cells were re-stimulated *ex-vivo* with 10uM SIINFEKL peptide for 5 hours in the presence of brefeldin-A (BD biosciences, 555029) for the last 4 hours. Secondary necrosis was induced by treating acR3-OVA cells or acC8-OVA cells with dimerizer at 100nM for 24hours prior to immunization. Mechanical necrosis was induced by three Freeze/thaw cycles (freeze in liquid nitrogen and thaw at 37°C) of acR3-OVA or acC8-OVA cells. Where indicated, cells were pre-treated with BAY-117805 (10 μ M) for 15min prior to cell death induction.

In conditions in which cells were induced to die by dsRNA, 10 μ g/ml of poly I:C was transfected using LipofectamineRNAiMAX (Life technologies). Indicated cell lines were transfected for 6 hours prior to immunization with 5×10^5 OVA expressing MEFs or 10^6 CT26 as described above.

In vivo cytotoxic assay. Immunized animals were adoptively transferred at day 8 with CFSE-labelled splenocytes and the frequency of CSFE^{hi} (irrelevant peptide control) and CFSE^{low} (SIINFEKL loaded) splenocytes was determined at day 9.

In vitro DC-dying cells co-cultures. For phagocytosis assay, bone marrow derived dendritic cells (BMDCs) were generated by GM-CSF differentiation. We aknowledge the lab of Acha-Orbea for the MuTuDC. MuTuDC are derived from WT C57BL/6 tumour-bearing transgenic

mice expressing the SV40LgT oncogene under the CD11c promoter and were cultured as described in (40). 5×10^5 BMDCs or MuTuDCs were plated in a tissue culture treated 12-well-plate in 500 μ L of RPMI complete media per well. Next, PKH-26 (PKH-26GL, Sigma Aldrich) stained cells (acC8-, acR3- and acR3 Δ C-expressing cells stained following the manufacturers protocol) were induced to die as described above and 5×10^5 dying cells were added in each well in 500 μ L RPMI complete media (1:1 ratio). At the indicated time points, cells were analysed by flow cytometry. The phagocytic index was calculated as the percentage of PKH-26 $^+$ cells in CD11c $^+$ gate and normalized by subtracting the percentage obtained at 4°C from that at 37°C at matched time points.

For DC maturation study, 5×10^4 BMDCs were plated in U-bottom 96 well plate (in triplicates) and dying cells were added at 1:1 ratio, as described above. At the indicated time points, cells were analysed by flow cytometry.

In vivo peritoneal inflammation. WT mice were injected with 200 μ L PBS or 2×10^6 dimerizer treated acC8-, acR3- and acR3 Δ C-expressing NIH-3T3 cells (in 200 μ L PBS) in the peritoneal cavity. At the indicated time points, mice were sacrificed and peritoneal cells were collected in 5 ml PBS.

Tumor growth *in vivo*. C57BL/6 J and BALB/c CBYJ mice were subcutaneously injected with 5×10^5 B16F10-OVA cells or 5×10^5 CT-26 cells, respectively. Tumor height and width were measured with a caliper every 2-3 days and tumor volume was calculated (*Elliptical volume* = $width^2 \times height \times 0.523$). For tumor protection experiments, 12 days or 7 days prior to challenge with B16F10-OVA or CT26 cells, mice were immunized with the indicated dying cells as described above. To read out immune responses induced by CT26 tumor cells, cell suspension from spleen and draining inguinal lymph node were plated in a U-bottom 96

well plate at 5×10^4 cells per well and restimulated with 5×10^3 CT26 cell lysates (heated 5 min at 42°C and 1 cycle of freeze/thaw in liquid nitrogen). 24hrs and 72hrs after restimulation, supernatants were collected and IFN γ was measured by ELISA (eBioscience). Mice were sacrificed when diameter reached 15mm.

Flow cytometry. Fluorochrome conjugated anti-mouse CD3e (clone 145-2C11), CD8a (clone 53-6.7), CD19 (clone ID3), IL-2 (clone JES6-5H4), TNF α (clone MP6-WT22), KLRG1 (clone 2F1), Granzyme-B (clone NGZB), CD45.2 (clone 104), I-A b (clone AF6-120.1), CD40 (clone HM40-3), CD86 (clone GL1), CD11c (clone N418), CD11b (clone M1/70), Cleaved-Caspase-3 (clone C92-605) (BD Biosciences), IFN- γ (clone XMG1.2) (e-biosciences), and anti-Calreticulin (Abcam) were used following the manufacturers protocol. Phosphatidylserine exposure was detected using Annexin V (BD Biosciences). For identification of membrane permeabilized dead cells, Live/Dead fixable reagent (Violet, Yellow and Aqua) (Life technologies) was used. For intracellular cytokines, staining was done following the manufacturer protocol using Cytofix/Cytoperm kit (BD Biosciences). For all staining protocols, cell suspensions were incubated in mouse Fc block (anti CD16/CD32 clone 2.4G2 BD Biosciences) prior to staining with markers antibodies. Flow cytometry was performed using a BD LSRII Fortessa. Analysis was done using FlowJo software (Treestar).

IncuCyte. Cell death assays were carried out using a 2-color IncuCyte Zoom in-incubator imaging system (Essen Biosciences, Ann Arbor, MI, USA) as described(21). Cell death was induced by treating cells with indicated reagents (B/B homodimerizer (Clontech-635069 ; mTNF α (peprotech-31501A) ; z-Vad-FMK (RD systems, FMK001) ; Necrostatin-1 (Merck Millipore-480065)) in a 12-well tissue culture plate (200 000 cells/well), in the presence of 1 μ M of membrane permeability dyes Yo-pro1 or Yo-pro3 (Life Technologies, Grand Island,

NY, USA; S7020). For each experiment, a minimum of three separate wells were treated for each experimental condition and a minimum of 4 image fields were assessed per well. TNF α , dimerizer, zVad and Nec-1 were used at a concentration of 50ng/ml, 100nM, 20 μ M and 30 μ M, respectively, throughout, unless indicated otherwise.

Measurement of analytes released by dying cells. acC8-, acR3- and acR3 Δ C-expressing NIH-3T3 cells were plated in triplicates in a flat-bottom 96 wells plate (5 \times 10 4 cells/well). Upon treatment with indicated drugs, culture supernatants were collected at different time points and freezed at -20°C until assay. Alternatively, WT and *ripk1* $^{-/-}$ MEFs were plated in 6-well plate (5 \times 10 5 cells/well) and pIC-transfected as indicated above, with the indicated concentrations. 8hrs and 24hrs later, culture supernatants were collected. Supernatants were processed with the Cytokine Mouse Magnetic 20-Plex Panel (Life technologies-LMC0006M) following the manufacturer protocol and analysed on a MagPix instrument (Luminex corporation). IL-6 (eBioscience 88-7064), IL-33 (eBioscience 88-7333), HMGB1 (IBL international ST51011) were measured by ELISA following the manufacturer's protocol. Fluorescence was read on a Multiskan Spectrum (Thermo Scientific). Similarly uric acid release was measured with the Uric acid Assay kit (Abcam, ab65344) with the fluorometric methods.

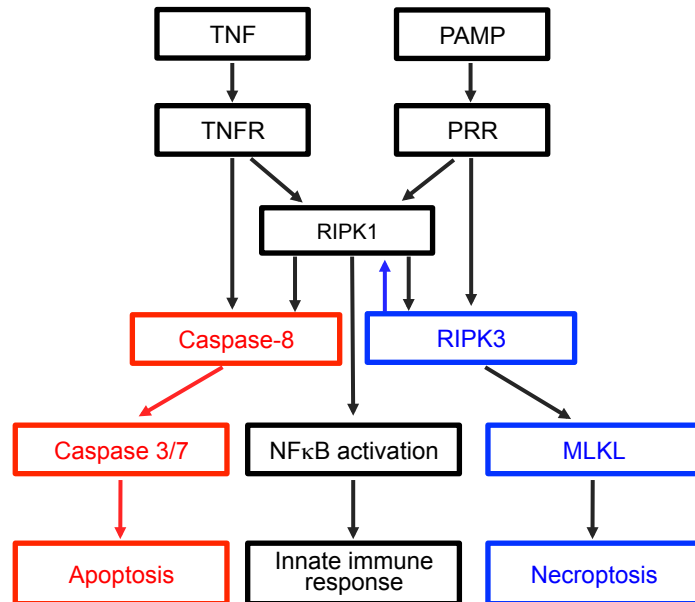
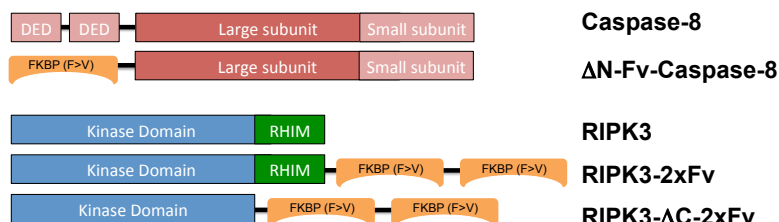
RNA extraction and gene expression analysis. acC8-, acR3- and acR3 Δ C-expressing NIH-3T3 cells were plated at 5 \times 10 5 cells in 6 well plates and induced to die with dimerizer. At the indicated time points, cells were harvested and RNA was extracted using the High pure RNA isolation kit (Roche-11828665001). RNA quantity was measured with Nanodrop and RNA quality was assessed in an Agilent 2100 Bioanalyser using the Agilent RNA 6000 total RNA nano kit. RNA samples were analysed by nCounter gene expression analysis and quantified with the nCounter Digital Analyser (Nanostring technologies). Expression of 179 genes was

analyzed using nCounter CX Mouse inflammation kit. Normalization was conducted with nSolver Analysis Software 1.1. Data were normalized using positive and negative controls and house keeping gene probes. Data visualization and statistical analysis were performed using the Qlucore Omics Explorer, v2.3 (Qlucore). Experiment was performed three independent times with all data shown. Hierarchical clustering was performed and gene sets were filtered for variance in order to exclude non-expressed or non-variable genes among the dataset. In Figure 3, RNA counts from each time point were normalized to corresponding untreated condition. In fig S4, absolute RNA counts were analysed by rank regression with respect to time, performed for each time series and each type of cell death. Genes that were significantly upregulated ($q < 0.05$) are shown.

Western Blot. Cells were lysed in Dulbecco's phosphate buffered saline (Life Technologies), 1% NP40, phosSTOP phosphatase inhibitors (Roche) and a complete protease inhibitor cocktail (Roche). Antibodies used for western blotting recognized RIPK1 (BD Biosciences), RIPK3 (Imgenex), I κ B α , phosphorylated ERK, ERK, phosphorylated p38 and p38 (Cell Signaling Technology, cat #9242, 9251, 9252, 4631 and 9212).

NF- κ B reporter assay. Cells in 6 well plates were transfected with 4 μ g NF κ BLuc plasmid (firefly luciferase) and 0.4 μ g control plasmid (renilla luciferase) using Lipofectamine 2000 (Life Technologies) for 6hrs, then replated in 12-well plates and transfected 16h later with pIC at the indicated dose for 8 hours. Cells were then lysed and luciferase was quantified using the Dual-Luciferase reporter assay system (Promega E1910).

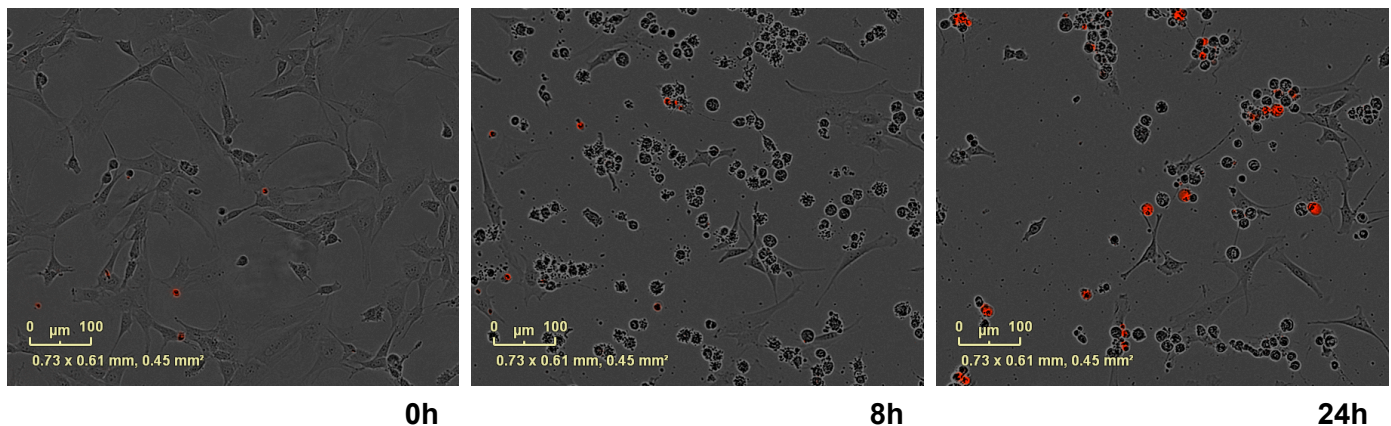
Statistical analysis. Statistical tests were preformed using Prism GraphPad v6.0. Analysis of nanostring data were performed using the Qlucore Omics Explorer, v2.3 (Qlucore).

A**B****Fig. S1.**

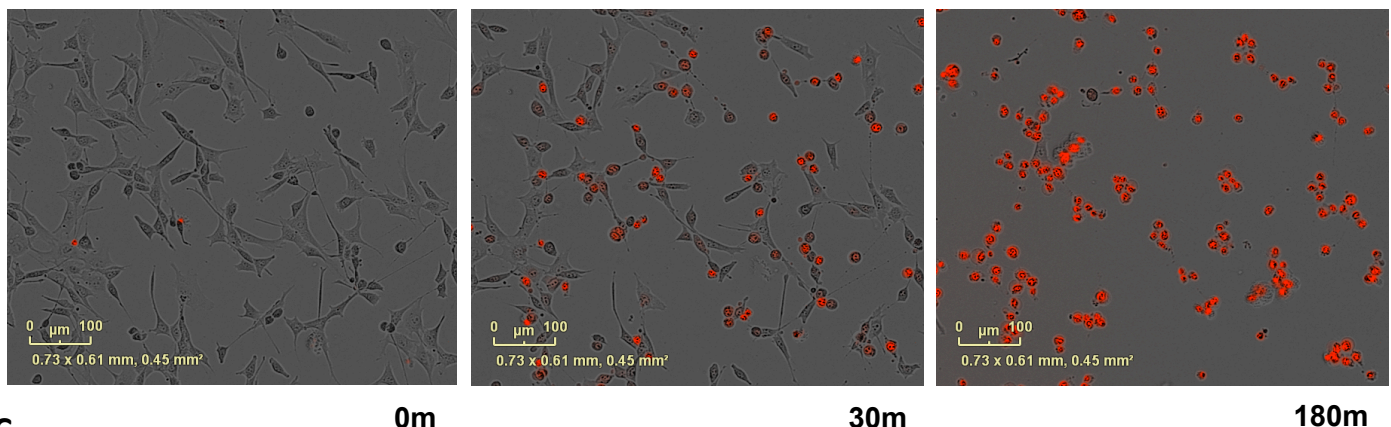
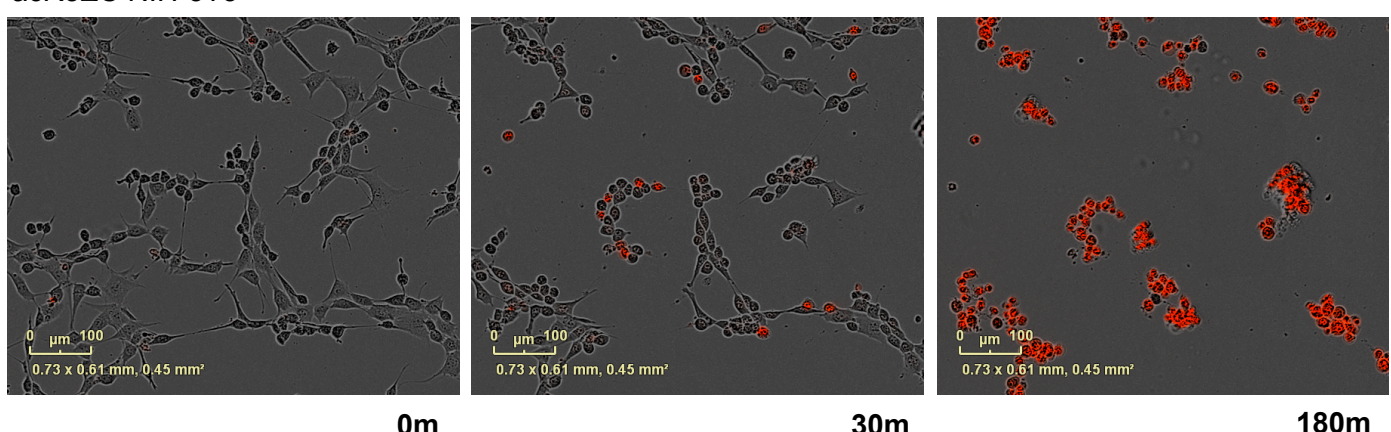
Engineering “pure” cell death systems. (A) Schematic representation of cell death and inflammatory pathways downstream of TNF-R and PRRs. Extensive investigations in the field of cell death and immunity over the past decade have challenged the dichotomy between apoptosis (regulated and non-inflammatory) as contrasted by necrosis (accidental and inflammatory). Several forms of regulated necrosis, such as necroptosis (RIPK3-dependent) and pyroptosis (caspase 1/11 dependent), are now recognized. Moreover, recent studies have revealed the ability of apoptotic cells to secrete pro-inflammatory cytokines(41), whereas necroptotic cell death can terminate TNF induced inflammation(42). In this context has emerged the notion that cell death and host defense pathways are intimately linked (18, 19). For example, RIPK1 has been shown to be crucial for NF- κ B activation downstream of several innate receptors, while it also regulates both caspase-8 and RIPK3 dependent cell death (39). Similarly, caspase-8 and RIPK3 contribute to inflammasome activation and IL-1 β release (43), while also being the effector pathways for apoptosis and necroptosis, respectively. (B) Schematic representation of dimerizable caspase-8 and oligomerizable RIPK3 constructs.

A

acC8 NIH-3T3

**B**

acR3 NIH-3T3

**C**acR3 Δ C NIH-3T3**Fig. S2.**

Dimerization of caspase-8 induces apoptosis and oligomerization of RIPK3 induces necroptosis.
(A-C) acC8-, acR3-, or acR3 Δ C-expressing NIH-3T3 cells were stimulated with dimerizer in the presence of Yo-pro3 and live cell imaging was performed using the IncuCyte. $N=3$, representative images at indicated time point are shown.

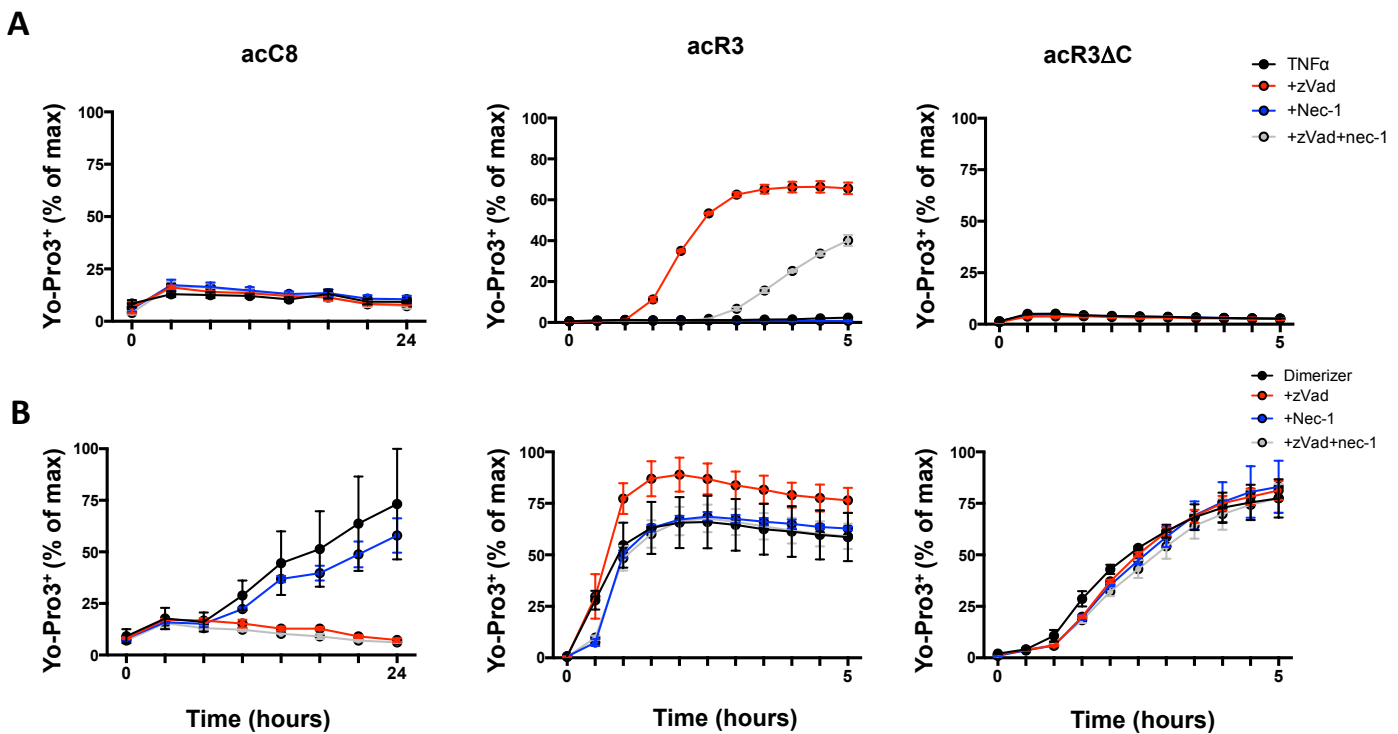


Fig. S3.

Kinetics of dimerizer and TNF α induced cell death. (A,B) acC8-, acR3- and acR3 Δ C-expressing NIH-3T3 cells were stimulated with TNF α alone (A) or dimerizer (B) in the presence of zVad and/or Nec-1. Yo-pro3 was added to all cultures and cell death was quantified in real time using the incucyte live imaging system. Number of positive red, Yo-pro3 objects per well were enumerated and plotted as a percentage of maximum cell death. NIH-3T3 cells do not express RIPK3 and are therefore resistant to tumor necrosis factor (TNF) α and zVAD induced necroptosis(17); expression of the RIPK3-2xFv construct (but not the RIPK3 Δ C-2xFv construct) sensitized the cells to TNF-induced necroptosis, indicating that the necroptotic cell death pathway was otherwise fully intact and that RIPK1 was indeed unable to engage RHIM-less RIPK3. $N=2$, mean values are shown from triplicate wells from one experiment and error bars indicate SEM

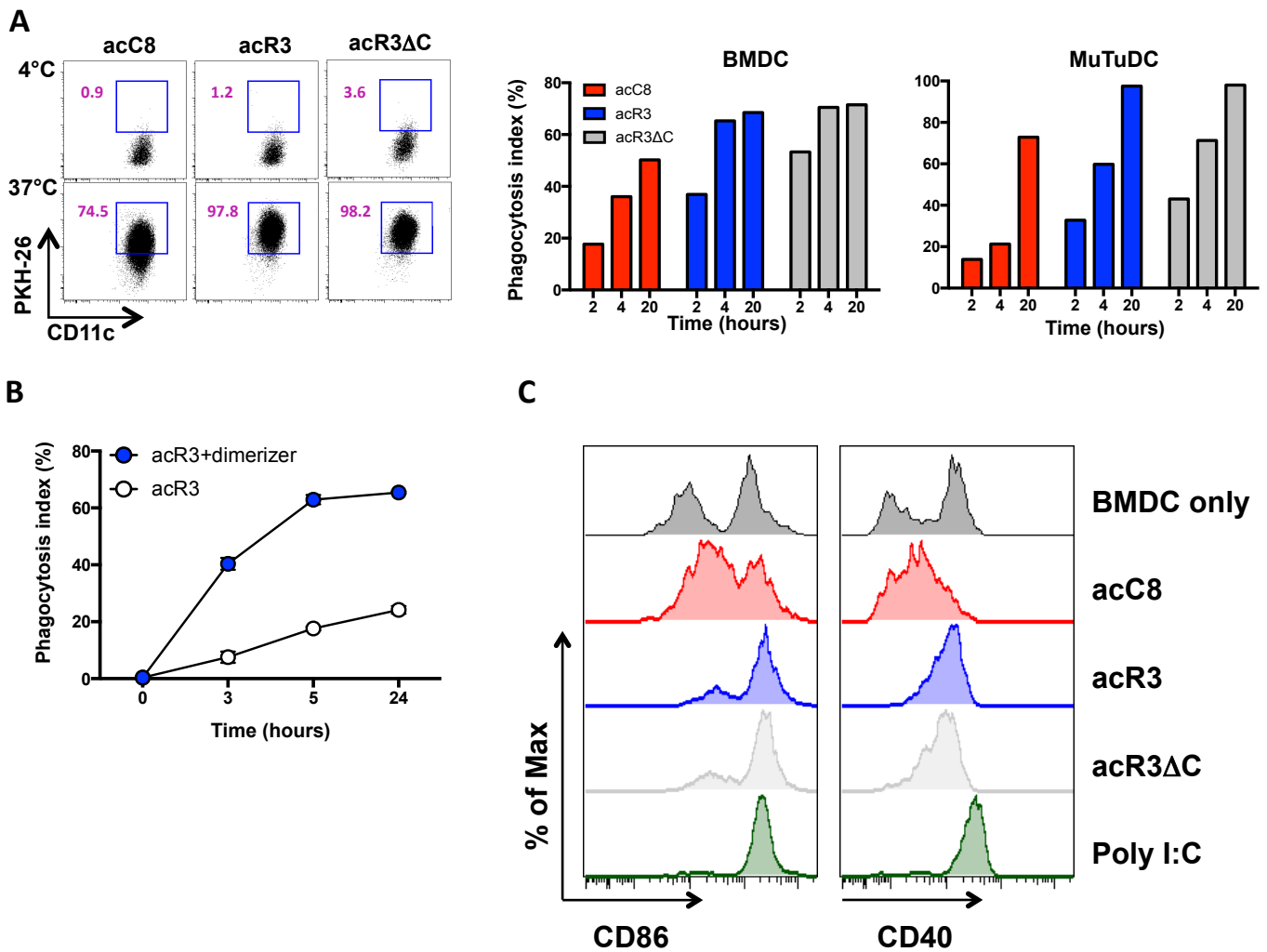


Fig. S4.

Dying cells trigger phagocytosis and activate dendritic cells (A) BMDCs or MuTu DCs were co-cultured with PKH26-labeled and dimerizer treated acC8-, acR3- or acR3ΔC-expressing cells. CD11c⁺ PKH26⁺ events were quantified by flow cytometry after 2, 4 and 20h. $N=2$, values are shown from one representative experiment- representative FACS plot (right) and histograms (left) (B) BMDCs were co-cultured with PKH26-labeled acR3 cells in the presence or absence of dimerizer. CD11c⁺ PKH26⁺ events were quantified by flow cytometry at the indicated time points. Mean values are shown from triplicate wells from one experiment and error bars indicate SEM (C) BMDCs were co-cultured with dimerizer treated acC8-, acR3-, acR3ΔC-expressing cells or treated with poly I:C (1 μ g/ml) for 24h and DC maturation phenotype was assessed by flow cytometry- representative FACS histograms are shown.

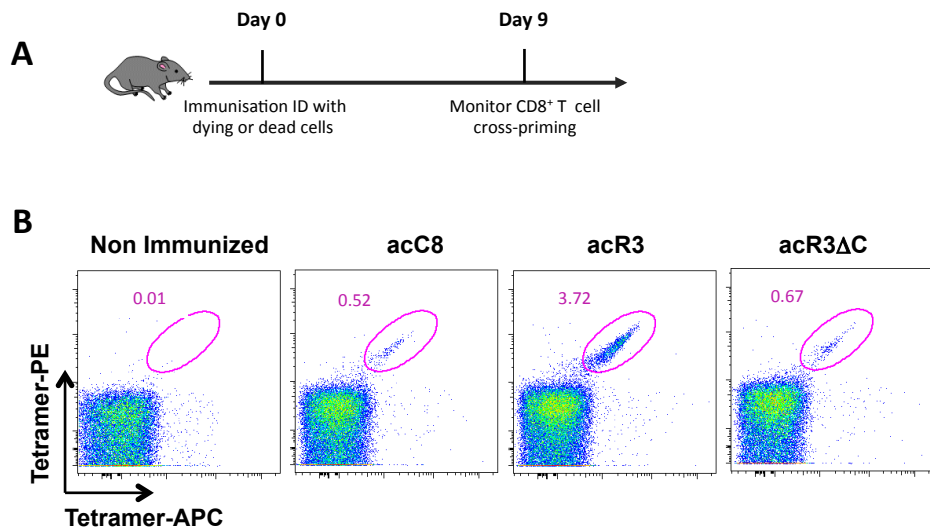


Fig. S5.

Monitoring CD8⁺ T cell cross-priming (A) Schematic representation of cross-priming assays using dying cells as a source of antigen. (B) Representative FACS plots for Fig. 2A.

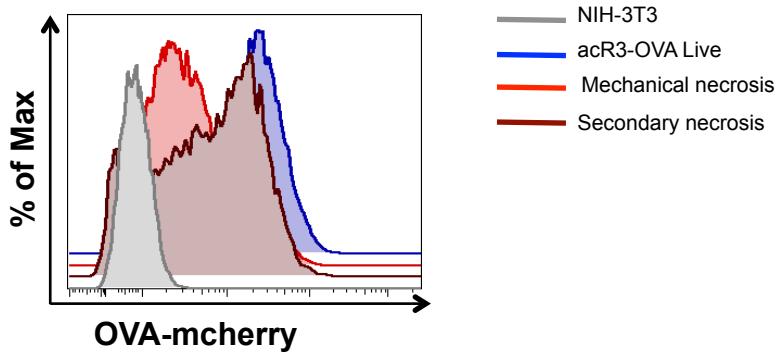


Fig.S6.

Partial antigen loss after necrotic membrane permeabilization. FACS histogram indicating OVA-mcherry mean fluorescence intensity in necrotic cells, as compared to live cells.

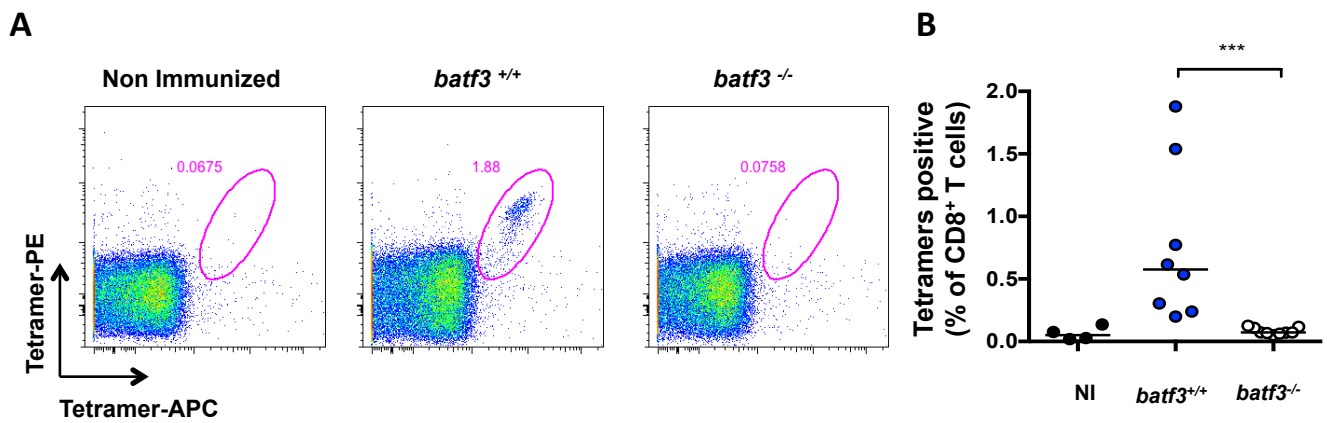
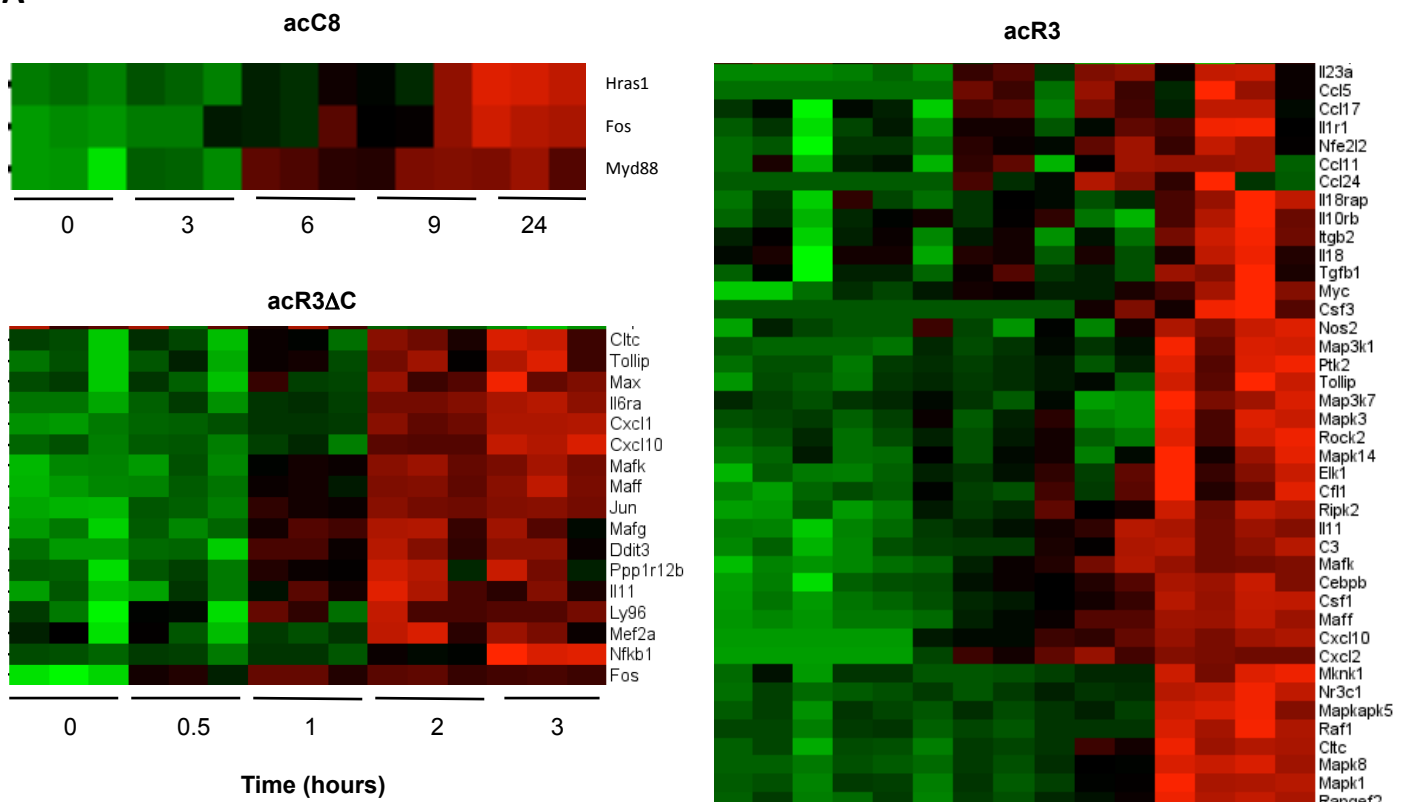
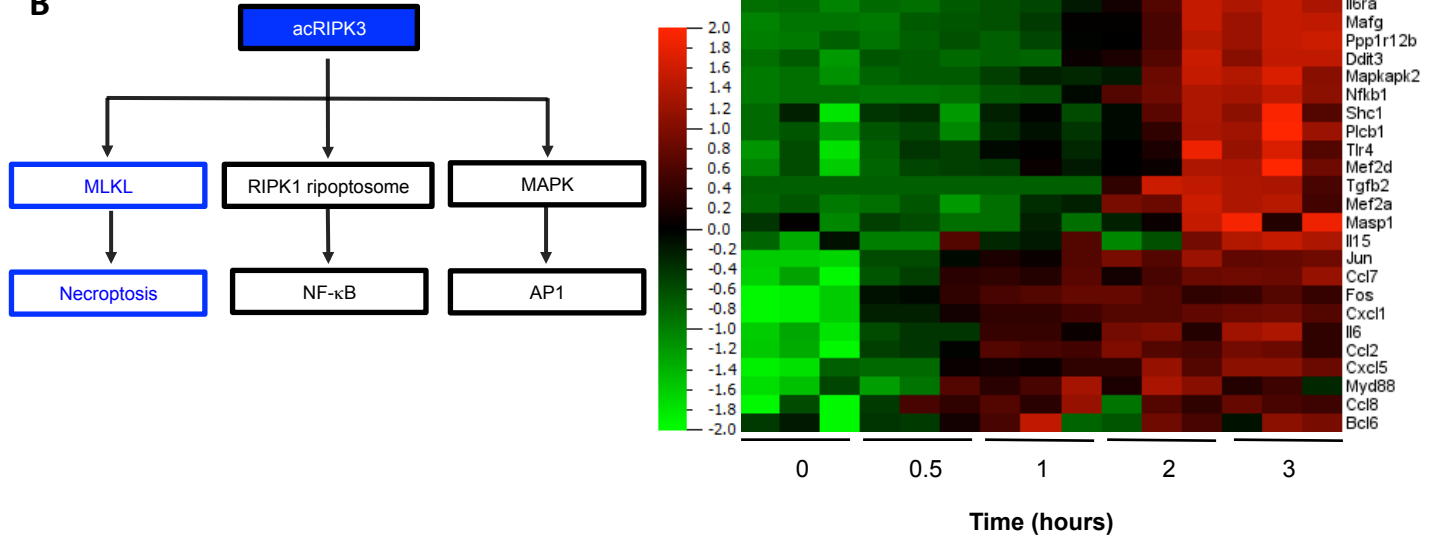


Fig. S7.

Necroptotic cells induced cross-priming of CD8⁺ T cells requires BATF3-dependent DCs. (A and B) Matched *Wt* and *Batf3*^{-/-} mice were immunized with acR3-OVA-expressing NIH-3T3 cells and OVA-specific CD8⁺ T cells were quantified using K^b-SIINFEKL-tetramers and plotted as a percentage of total CD8⁺ T cells, $N=2$. (A) Representative FACS plots are shown, (B) Represented data are pooled from two independent experiments with 4 mice per group, bars indicate median.

A

Time (hours)

B**Fig. S8.**

Oligomerization of full-length-RIPK3 induces a strong inflammatory transcriptional signature. (A) acC8-, acR3- and acR3ΔC-expressing NIH-3T3 cells were induced to die with dimerizer, and at indicated time points RNA was extracted for transcriptional profiling. Hierarchical clustering was performed on the data set obtained from Nanostring inflammation codeset analysis. Absolute RNA counts were analysed by rank regression with respect to time, performed for each time series and each type of cell death. Genes that were significantly upregulated ($q < 0.05$) are shown and listed in **Table S1**. Heat map indicates the relative expression of the indicated transcript (red indicating high levels of expression, green indicating low levels of expression). (B) Schematic representation of inflammatory pathways triggered downstream of RIPK3 activation. q -values (false discovery rate or FDR-adjusted p -value) were determined using Qlucore Omics. $N=3$, shown data are pooled from three independent experiments.

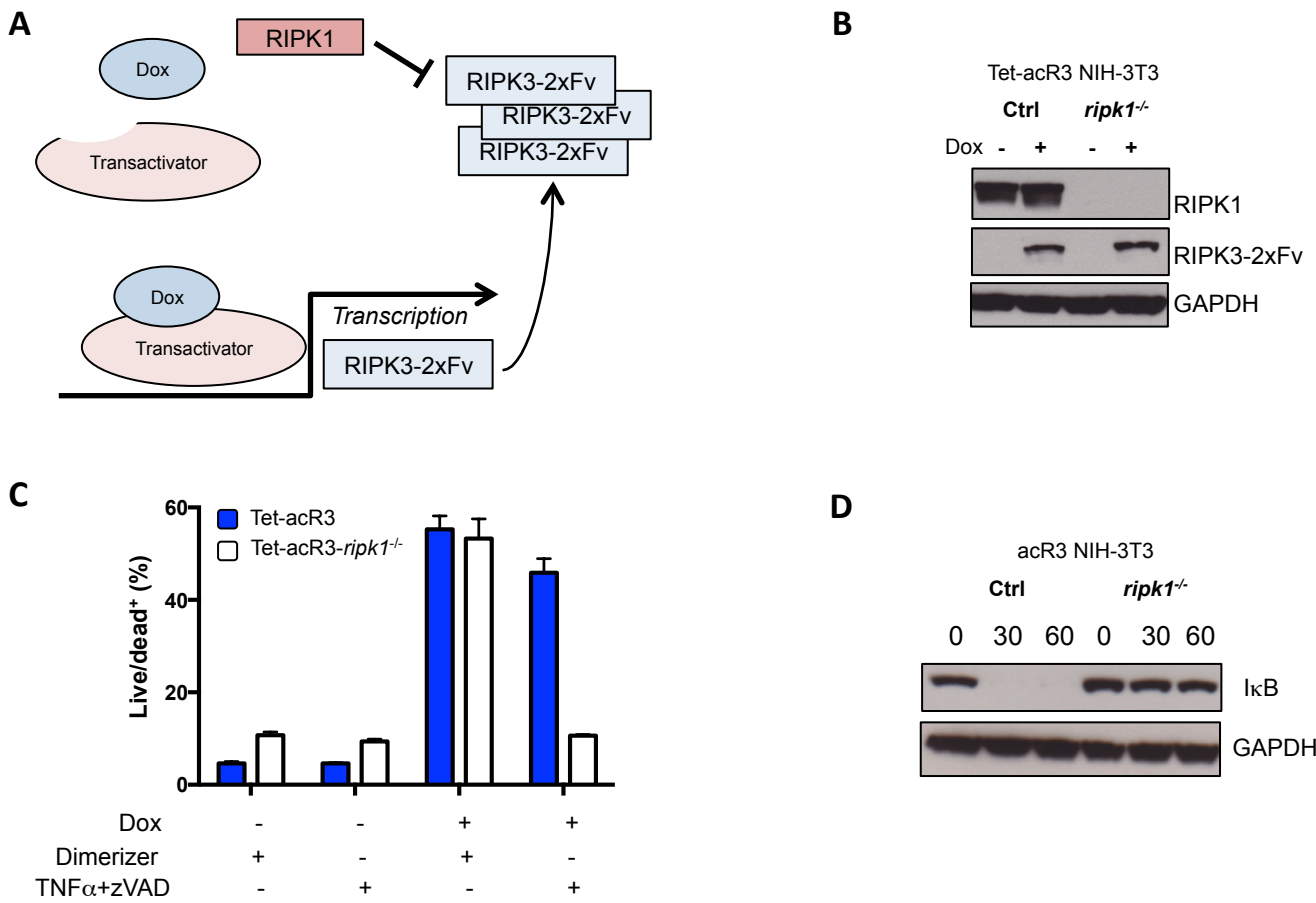


Fig. S9.

Deletion of *ripk1* in acR3-expressing NIH-3T3 cells abolishes NF- κ B activation. (A) Constitutive RIPK3 expression in cells lacking RIPK1 is toxic to the cells because RIPK1 has a suppressive effect on spontaneous RIPK3 activation (21, 23). Thus, we expressed RIPK3-2xFv under a doxycycline (Dox) inducible promoter. (B) Protein extract from Ctrl and *ripk1*^{-/-} Tet-acR3 NIH-3T3 cells were analysed by Western Blot in order to confirm CRISPR-cas9 gene editing. Cells were also treated overnight with Dox at 500ng/ml to confirm inducible expression of RIPK3-2xFv construct. (C) Tet-acR3 and Tet-acR3 *ripk1*^{-/-} cells were treated for 6hours with dimerizer (100nM) or TNF α (50ng/ml) and zVAD (50 μ M) and analysed by flow cytometry with a membrane permeability dye (live/dead) . Histogram represent mean +/-SEM of triplicates. (D) Protein extract from Ctrl and *ripk1*^{-/-} acR3 NIH-3T3 cells were analysed by Western Blot in order to analyse I κ B degradation upon treatment with dimerizer.

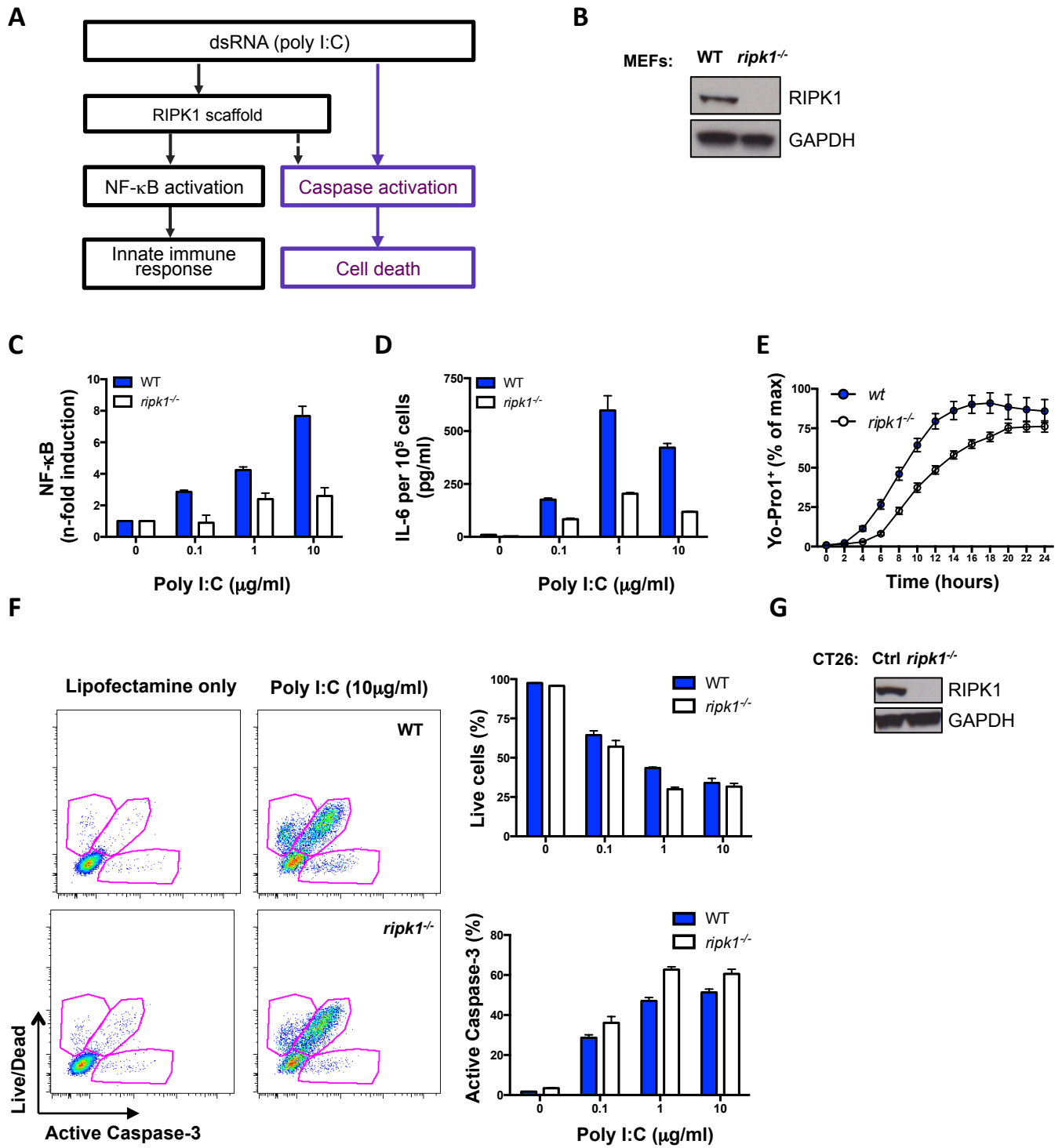


Fig. S10.

Deletion of RIPK1 abrogated poly I:C-mediated NF-κB activation and cytokine production from apoptosis. (A) Schematic representation of poly I:C induced cell death and NF-κB signaling. (B) Protein extracts from WT and *ripk1*^{-/-} mouse embryonic fibroblasts (MEFs) were analysed by Western blot. (C) WT and *ripk1*^{-/-} MEFs were transfected with NFκB-Luc plasmid for 24hours; followed by treatment with the indicated amount of poly I:C for 8h before cells were collected and luciferase activity quantified. (C) Cells were transfected with poly I:C at the indicated amounts, and supernatants collected 8h later for IL-6 quantification. (D) WT and *ripk1*^{-/-} MEFs were transfected with poly I:C (10mg/ml) in the presence of Yo-Pro1 and cell death was monitored using real-time imaging. (E) Cells were transfected with poly I:C at the indicated amounts and collected 24hours later and analysed by flow cytometry for caspase-3 activation—representative FACS plots are shown (left) and quantification histograms (right). (C to F) N=2, histograms represent mean +/- SEM of triplicates from one experiment. (G) Protein extracts from CT26 Ctrl or a CRISPR/cas9-modified line that lacks RIPK1 expression (CT26 *ripk1*^{-/-}) in order to confirm efficient *ripk1* deletion.

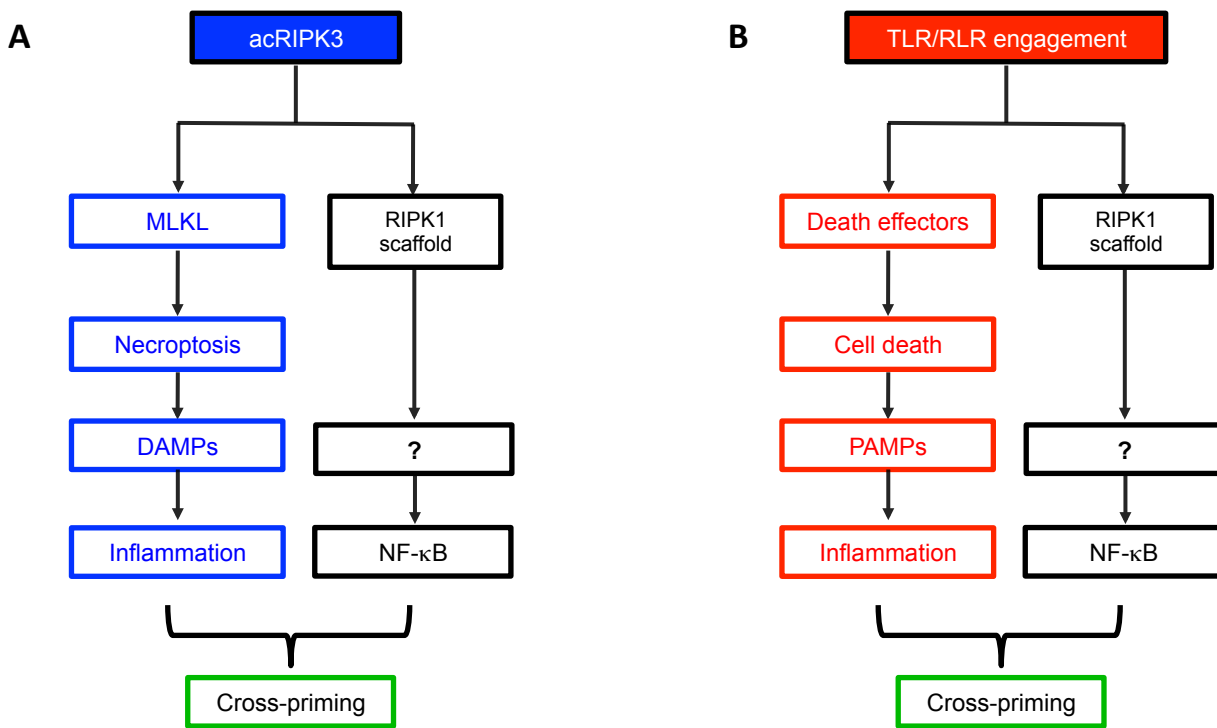


Fig. S11.

Proposed model for the regulation of cross-priming of CD8+ T cells by dying cells. Our study demonstrate that coordinated cell death and NF-κB activation within dying cells determines their cross-priming potential. Using an inducible dimerization system to trigger RIPK3-necroptosis in sterile conditions (A), we have shown that RIPK3 was able to recruit RIPK1 via its RHIM domain, resulting in the activation of an NF-κB transcriptional program. Uncoupling NF-κB activation from RIPK3-necroptosis did not affect their ability to release DAMPs, activate dendritic cells, nor to induce the recruitment of immune cells into the peritoneal cavity. However, we found that immunogenicity of dying cells was dependent on RIPK1 signaling and NF-κB activation. Similarly, immunogenicity of cytosolic double-stranded (ds)RNA (poly I:C) induced cell death was also regulated by the RIPK1-NF-κB axis within the antigen donor cell (B). Our results suggest a model whereby dendritic cells are able to sense the activation of innate immune signaling within dying cells, in turn regulating cross-priming of CD8+ T cells. The manner by which RIPK3 oligomerization mediated RIPK1-dependent NF-κB activation remains unclear. In contrast to TNFRI mediated NF-κB activation that is dependent on complex I formation (44-46), RIPK3 oligomerization forms a cytosolic complex that recruits RIPK1 via RHIM domain interactions, and caspase-8(21). Thus, the so-called RIPK3-necrosome is spatially and structurally similar to complex II (or the riopontosome), whose core components are RIPK1, FADD, Caspase-8 and FLIP(16, 17) reminiscent of NF-κB activation downstream of PRRs such as TLR3/4, DAI and RIGI/MDA5 (17, 31, 47, 48).

A acR3 NIH-3T3			B acR3ΔC NIH-3T3		
Transcript	p value	q value	Transcript	p value	q value
Cxcl1	4,51E-08	3,24E-06	Il6ra	1,83E-07	9,94E-07
Ccl7	7,79E-07	2,80E-05	Jun	5,90E-08	9,94E-07
Cebpb	1,28E-06	3,08E-05	Maff	2,34E-07	9,94E-07
Cxcl10	2,57E-06	4,38E-05	Mafk	2,24E-07	9,94E-07
Mafk	3,04E-06	4,38E-05	Cxcl1	5,56E-06	1,89E-05
Ccl2	8,26E-06	5,95E-05	Max	1,95E-05	4,74E-05
Cxcl2	7,34E-06	5,95E-05	Tollip	1,89E-05	4,74E-05
Cxcl5	6,42E-06	5,95E-05	Cxcl10	2,35E-05	4,99E-05
Jun	6,70E-06	5,95E-05	Cltc	3,76E-05	7,11E-05
Maff	7,89E-06	5,95E-05	Ddit3	7,26E-05	1,23E-04
Mapkapk2	1,19E-05	7,78E-05	Mafg	1,60E-04	2,26E-04
Csf1	1,82E-05	9,33E-05	Nfkbp1	1,50E-04	2,26E-04
Il6ra	2,07E-05	9,33E-05	Ly96	3,43E-04	4,49E-04
Myc	1,96E-05	9,33E-05	Ppp1r12b	7,81E-04	9,48E-04
Nfe2l2	1,84E-05	9,33E-05	Il11	9,52E-04	1,08E-03
Nfkbp1	1,94E-05	9,33E-05	Fos	1,13E-03	1,20E-03
Mef2d	2,68E-05	1,14E-04	Mef2a	2,63E-03	2,63E-03
Tlr4	4,37E-05	1,75E-04			
Cltc	4,94E-05	1,87E-04			
Plcb1	5,68E-05	2,05E-04			
Masp2	7,02E-05	2,30E-04			
Mef2a	7,10E-05	2,30E-04			
Ripk2	7,36E-05	2,30E-04			
Il11	8,85E-05	2,38E-04			
Mafg	8,94E-05	2,38E-04			
Ppp1r12b	8,50E-05	2,38E-04			
Shc1	8,65E-05	2,38E-04			
Ddit3	1,02E-04	2,62E-04			
Hdac4	1,09E-04	2,71E-04			
Mapk8	1,14E-04	2,73E-04			
Rps6ka5	1,35E-04	3,14E-04			
Rapgef2	1,62E-04	3,65E-04			
Mapk1	1,75E-04	3,81E-04			
C3	1,85E-04	3,88E-04			
Tgfb2	1,89E-04	3,88E-04			
Il6	2,12E-04	4,24E-04			
Nr3c1	2,20E-04	4,28E-04			
Il1r1	2,82E-04	5,35E-04			
Mapkapk5	3,06E-04	5,64E-04			
Max	4,23E-04	7,62E-04			
Tollip	4,42E-04	7,76E-04			
Il18rap	4,71E-04	8,08E-04			
Raf1	5,99E-04	1,00E-03			
Mknk1	6,93E-04	1,13E-03			
Map3k1	7,78E-04	1,24E-03			
Fos	9,19E-04	1,43E-03			
Ptk2	9,35E-04	1,43E-03			
Ccl5	1,03E-03	1,54E-03			
Il23a	1,09E-03	1,61E-03			
Elk1	1,44E-03	2,08E-03			
Nos2	1,80E-03	2,54E-03			
Masp1	1,90E-03	2,63E-03			
Il15	2,08E-03	2,82E-03			
Ccl17	2,12E-03	2,83E-03			
Csf3	2,21E-03	2,89E-03			
Itgb2	2,31E-03	2,92E-03			
Tgfb1	2,31E-03	2,92E-03			
Rock2	3,63E-03	4,50E-03			
Cfl1	4,97E-03	6,07E-03			
Il10rb	6,48E-03	7,65E-03			
Mapk14	6,44E-03	7,65E-03			
Ccl8	6,93E-03	8,04E-03			
Il18	7,27E-03	8,30E-03			
Mapk3	8,59E-03	9,67E-03			
Ccl11	9,95E-03	1,10E-02			
Ccl24	1,02E-02	1,12E-02			
Myd88	1,05E-02	1,13E-02			
Bcl6	1,25E-02	1,33E-02			
Map3k7	1,32E-02	1,37E-02			
Limk1	1,99E-02	2,04E-02			
Tradd	2,08E-02	2,11E-02			
Ly96	2,86E-02	2,86E-02			

Table S1.
Complete list of transcripts that are significantly upregulated during necroptosis (q<0.05). Absolute RNA counts from acR3 and acR3ΔC- expressing cells time series were analysed by rank regression in respect to time. Genes that were significantly upregulated (q<0.05) are listed for acR3 (A) and acR3ΔC (B) with corresponding p and q values (hierarchical clustering is shown in fig. S8).

Movie S1

acC8-expressing NIH-3T3 cells were treated with 100nM dimerizer in the presence of Yo-Pro3 (1 μ M) and cell death was imaged every 30 minutes for 24 hours using the IncuCyte imaging system

Movie S2

acR3-expressing NIH-3T3 cells were treated with 100nM dimerizer in the presence of Yo-Pro3 (1 μ M) and cell death was imaged every 5 minutes for 3 hours using the IncuCyte imaging system

Movie S3

acR3 Δ C-expressing NIH-3T3 cells were treated with 100nM dimerizer in the presence of Yo-Pro3 (1 μ M) and cell death was imaged every 5 minutes for 3 hours using the IncuCyte imaging system